Al-Azhar Bull. Sci. Vol. 24, No. 2 (Dec.): pp. 37-52, 2013.

HYDROTHERMAL SYNTHESIS AND CHARACTERIZATION OF NANO SIZED ZSM-5 AND THEIR EFFECT ON THE DECOLORIZATION OF INDIGO CARMINE DYE

IBRAHEEM OTHMAN ALI, IBRAHEM ALI IBRAHEM, KARAM SAIF ELNASSER
Department of Chemistry, Faculty of Science, Al-Azhar University, Nasr City 11884, Cairo, Egypt
** Corresponding author. Tel.: +202 22629357/8; fax: +202 22629356.*
E-mail address: Ibraheem_othman2002@yahoo.com (I. Othman).

Abstract

Silica sources can influence different effects of ZSM-5 crystallization and it leads to change in the properties of the final product. The crystallinity of nanosized ZSM-5 zeolite from precursors mixtures containing different silica sources, e.g. tetraethylorthosilicate (TEOS), colloidal silica (CS), silicic acid(SA) and fumed silica(FS) have been studied. The produced samples are investigated using XRD, SEM, FT-IR, pyridine adsorption and N_2 adsorption measurements. XRD results show that the product obtained by different silica sources is nano sized ZSM-5 phase. SEM results show that silica sources influences on shape of the produced ZSM-5; the sample which was prepared by silicic acid crystallized in spherical shape crystals, the samples which was prepared by TEOS crystallized in cubical shape crystals, the sample which was prepared by colloidal silica crystallized in spherical shape crystals with smaller aggregated but the sample which was prepared by fumed silica crystallized in round shape crystals. N_2 adsorption results show that silica sources influences on pore diameter and pore volume of the produced ZSM-5.The adsorption of indigo carmine dye by ZSM-5 has been studied. It was found that the synthesized zeolite by SA exhibited significantly higher adsorption capacity for indigo carmine than other ZSM-5 states due to the difference in morphological properties. The optimum ZSM-5 loading is 1 g at pH 4 after 180 min.

Keywords**: ZSM-5; Hydrothermal synthesis; Silica sources; Physicochemical properties.**

1. Introduction

The colour of wastes is the most apparent indicator of waste pollution and it should be reduced before their drop. The presence of small amounts of dyes (below 1 ppm) is clearly visible and considerably influences the water environment. Removing colour from wastes is often more important than other colorless organic substances [1]. Indigo carmine (IC) is one of the oldest dyes and still one of the most important used. Its major industrial application is the dyeing of clothes (blue jeans) and other blue denim [2]. It has also been employed as redox indicator in analytical chemistry and as a microscopic stain in biology.

Several studies have been made on the oxidation kinetics of IC using peroxydisulfate, hypohalides and N-haloarenesulfonamides agents [3,4]. The

oxidation of IC by H_2O_2 in the presence of some sulfur compounds, such as sulfide, thioacetamide, thiourea and thiosulphate has been investigated [5]. Moreover, the homogeneous catalytic activity of transition metal ions for the oxidation reaction of IC and their kinetic determination has been studied [6,7]. Recent investigations revealed that reactive dyes could be decolorized by advanced oxidation processes (AOPs). These ambient temperature processes refer to the generation of highly reactive hydroxyl radicals that are aggressively and almost indiscriminately attack all types of inorganic and organic pollutants found in wastewater [8,9].

Zeolites are a series of microporous materials with pore size in the range of 0.3 nm to 1 nm and have been widely used as catalysts, adsorbents and ion-exchangers [9]. These open framework aluminosilicate solids are synthesized from a gel or solution containing appropriate amount of silica, alumina, water and alkali cations under hydrothermal conditions. The phase purity, crystal morphology and the reaction time are found to be very sensitive to the reactants, and in particular depend on the Si and Al sources [10]. A large variety of silicon sources with different characteristics, such as particle size, impurity and solubility in alkaline mixtures, have been used in zeolite syntheses [10].

It has been shown that silicon sources influence the formation of various silicate intermediates that may control the nucleation and crystallization processes, resulting in different properties of final crystals. Therefore, studying the effects of the silicon source on the zeolite formation will allow us to understand the mechanism of zeolite crystallization, especially the nucleation process, and control the characteristics of final products, such as crystal size, morphology and chemical composition.

Recently, interests in the synthesis of zeolite nanocrystals have grown continuously due to the several novel applications such as hosts of photochemically or optically active guests [11–13], seeds of thin film [14], adsorption of heavy metals and chromate [15,16] and chemical sensor [17]. Several zeolites, such as MFI, LTA, FAU, BEA, SOD and MEL, have been prepared in the form of colloidal suspension with narrow particle size distribution from clear homogeneous solutions [18]. The synthesis of zeolite crystals with equal particle radius requires homogeneous distribution of the viable nuclei in the system. Therefore, the homogeneity of the starting system and simultaneity of the events leading to the formation of precursor gel particles and their transformation into crystalline zeolitic material is of primary importance. In order to obtain such homogeneous starting systems abundant amounts of tetraalkylammonium hydroxides and water were employed [19-22]. On the other hand, the content of alkaline cations is very limited. All these factors together with the careful choice of the reactants allow the stabilization of starting mixtures where only discrete gel particles are presents [23–27]. The effect of different silica sources, which could play an important role in the formation of nanosized zeolites crystals, has not been investigated in detail. Most of the investigations were devoted to the synthesis of nanosized zeolites with tetraethylorthosilicate (TEOS) as a silica source. A limited number of articles

discuss the formation of nanosized zeolites by using other silica sources [28–31]. New data on the effect of silica in the synthesis of zeolite nanocrystals could be helpful in the fine-tuning of the ultimate size of the nanoparticles.

The aim of the present study was to investigate the effect of different silicon sources on the crystallization process and ultimate size of nanosized ZSM-5 crystallites. Hence, the synthesis of ZSM-5 by different silica source was characterized by X-ray diffraction, FT-IR, N_2 adsorption, SEM and acidity determination by pyridine adsorption. The investigation clearly shows that the silicon source has large influence on the nature of the precursor particles and species presenting in the early stages of the crystallization which in turn affects the growth process and the final morphology of the crystalline products. Finally, the decolorization of indigo carmine in the absence of UV irradiation is investigated for all prepared samples.

2. Experimental

The silica sources used for the preparation of the precursor mixtures were: tetraethylorthosilicate (TEOS, 98%, Fluka), colloidal silica; sodium metasilicate (30 wt.% SiO_2, Aldrich), fumed silica (Aldrich) and silicic acid (Fluka). The alkaline source was sodium hydroxide pellets (A.R 98%) and template source employed was cetyltrimethyl ammonium bromide (CTAB)

Indigo Carmine dye (C.I.73015) [3,3'-Dioxo-1,3,1',3'-tetrahydro-[2,2']-bi-indolylidene-5,5'-disulfonic acid disodium salt] was delivered from the general chemical company limited, Wembley Middlesex-England.

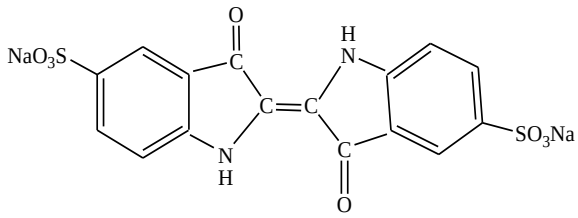

M.F. $C_{16}H_8N_2Na_2O_8S_2$, M.Wt. 466.35g/L. The peak intensity is at 608 nm; molar absorbtivity is 6309 mol^{-1} cm^{-1}.

2.1. Synthesis of nanosized ZSM-5

Nanosized ZSM-5 crystals were synthesized from a colloidal mixture having the following chemical composition:

$$3{:}21Na_2O{:}\ 0{:}162Al_2O_3{:}\ 6{:}185SiO_2{:}\ 0{:}185TPA{:}\ 100H_2O$$

The precursor mixtures were prepared by added1.1 g of NaOH dissolved in 10 ml of distillated water to appropriate amount of silica sources in 100 ml of distillated H_2O (but TEOS in ethanol) with stirring. The mixture was allowed to stir at ambient

temperature followed by heating at 80ºC until a clear solution of sodium silicate was obtained (solution A). Then, 2.2 g of CTAB was dissolved in 10 ml distillated water under stirring for 20 min (solution B). Both solutions (adding B–A) are stirred for 15 min. The aluminum sulfate (0.5 g), on the other hand, was dissolved in 10 ml of distillated water while adding 0.05-ml of concentrated H_2SO_4 under stirring until a clear solution reached. To the latter solution, the mixture of sodium silicate (solution A) and CTAB (solution B) was added followed by stirring for 30 min. The pH of the mixture was adjusted at 11 by using NaOH (0.1 M) and H_2SO_4 (0.1 M) solutions. Thereafter, the gel was transferred into an autoclave to a hydrothermal treatment under autogenous pressure at 100ºC, for a period of 72 h. The autoclaves were removed from the oil bath and quenched immediately with cold water. The solid product was filtered and washed with distilled water until pH of the filtrate dropped to eight. All products were dried at 120ºC for 3 h before calcination at 550ºC for 6 h in an oven, the sample prepared with fumed silica, colloidal silica, silicic acid and TEOS, are referred to S1, S2 S3 and S4, respectively.

2.2. Characterization techniques

2.2.1. X-ray diffraction (XRD)

Phase purity and crystallinity were determined by conventional powder X-ray diffraction (XRD) using a Philips diffractometer (type PW 3710). The patterns were run with Ni-filtered copper radiation (CuKα=1.5404 Å at 30kV and 10 mA) with a scanning speed of $2\theta = 2.5^{o}min^{-1}$. The mean particle size was calculated using the Debye–Scherrer Eq. (1) [32], in which K is a constant equal to 0.9, λ is the wavelength of the CuKα radiation, β is the half peak width of the diffraction peak in radiant and θ is the Bragg scattering angle.

$$D = k\lambda\backslash\beta \cos\theta \qquad (1)$$

The instrument line broadening was corrected using a LaB_6 as an internal standard. The crystallinity ratio of the prepared samples was calculated using the ratio of the sum of the areas of the five most intense peaks for the prepared samples (2θ = 8-10 and 23-24º) to those of corresponding peaks for the standard Na-ZSM-5 Mobil chemicals.

2.2.2. FT-IR spectra

FT-IR spectra were recorded on a Perkin Elmer Spectrum (RXI FT-IR) system, single beam spectrometer with a resolution of $2cm^{-1}$. The samples were ground with KBr (1:100ratio) as a tablet and mounted to the sample holder in the cavity of the spectrometer.

2.2.3. Nitrogen adsorption

The nitrogen adsorption isotherms of various zeolitic solids were measured at-196ºC using conventional volumetric apparatus. Prior to the determination of the adsorption isotherm, the sample (0.1g) was outgassed at 300ºC for 3h under a reduced pressure of 10^{-5}Torr in order to remove moisture. The specific surface area

(S_{BET}) was obtained using the BET method while the micropore volume (V^{μ}_{P}) and the external surface area (S^{ext}) were obtained from the "t-plot" method. This method was applied in order to have another estimation of the microporous volume that can be determined by the method developed by de Boer et al. [33].

2.2.4. Scanning electron micrographs (SEM)

Scanning electron micrographs were obtained using a Joel scanning microscope model JSM5410. Samples were deposited on a sample holder with an adhesive carbon foil and sputtered with gold.

2.2.5. FT-IR spectra of pyridine adsorption

The FT-IR spectral changes of Pyridine adsorption were measured in the 1700~ 1400 cm^{-1} region. Pyridine (5 Torr) was admitted into the cell and equilibrated with the sample for 30 min. Excess pyridine was then pumped out at 150ºC before recording the spectra. . The sample was pressed into a self-supporting water and mounted in a quartz infrared cell with CaF_2 windows connected to a reduced pressure of $l0^{-5}$ Torr closed circulating Pyrex system with a dead volume of $301cm^3$. The vacuum system was equipped with a vacuum gauge and the experiments were conducted when it leveled to 10^{-5} Torr. The infrared cell was equipped with an electric furnace and the sample temperature was adjusted by using the temperature controller connected to a thermocouple made of nickel chrome. The FT-IR sample was prepared by pressing the catalyst powder ground in an agate mortar to a wafer of ca 30 mg cm^2. All FT-IR measurements were carried out at room temperature. All the recorded spectra were presented by subtraction of the corresponding background reference.

2.3 Investigation of the adsorption activity

Adsorption studies were conducted using the batch method. Equilibrium isotherms were determined by contacting a given mass of adsorbent contained in glass bottles with 100ml of dye solution and 10ppm concentration. The pH of the fresh solution was adjusted using HCl and NaOH (pH 2, 4, 8, and 10). The precipitation of free acid dyes will occurred after dissolved of indigo carmine dyes in concentration of acid and lift for two days[34]. The bottles were subsequently sealed and stored at room temperature for various time lengths. It was found that an equilibrium time of 3 h was sufficient for each dye system studied. After this time the samples were filtrate and the concentration of dye was analyzed by a Perkin Elmer Instrument Lambada 35 at a band width of 2 nm. The spectra were measured at the maximum absorbance wavelength (608nm). The IC decolorization (C%) was considered in percent as:

$$C\% = \{(C_0 - C)/C_0\}\ x\ 100$$

3. Result and discussion

3.1 X-ray diffraction

XRD was employed to explore the phase composition and concentration of the constituent phases and to perform a refinement of the MFI unit cell parameters of the prepared samples. The XRD patterns (Fig. 1) of the ZSM-5 nanocrystals show five diffraction peaks in all samples characteristic of a zeolites with MFI topology in the 2θ region of 5°~45°. No other peaks could be observed for the ZSM-5 samples prepared by different silica sources, indicating a high purity of the products. The XRD crystallinity results were shown in Table 1. The results showed that the nature of silica source under the same crystallization conditions have a strong effect on the product purity. It should be noted that TEOS type silica contains ethanol as stabilizer that may act as template during the crystallization. The calculated values of the zeolite unit cell parameters for the ZSM-5 samples with different silica source agree well with the literature [35]. From the change in the unit cell parameters and the unit cell volume, it was found that change silica source leads to a series of well-regulated changes, including a progressive increase in the values of the α and the β angles and a decreased value of c. These changes may be due to the deformation of the unit cell when change silica source lead to change Al concentration in the lattice is increased. Moreover, the gradual diminishing of the lattice volume indicates a decreased micropore volume and pore mouth size.

3.2. Scanning electron micrographs (SEM)

Fig. 2 shows SEM image of crystals obtained from samples prepared by using different silica sources as FS, TEOS, CS and SA. Although the size of crystals produced with silicic acid (SA) was small, crystal shape can be clearly viewed and the crystal faces can be separately seen. The discrete single crystals obtained from SA are rounded-edged hexahedrons. The aspect ratio of crystals is nearly one. By keeping the batch composition the same, change of silica source from silicic acid to tetraethylorthosilicate leads to the formation of hexagonal twinned crystals with larger size and hemispherical raspberry when change silica by FS or CS. The chemical composition of the prepared samples was measured by EDX techniques summarized in Table 2. The results show that the Si/Al atomic % at three areas is almost similar and hence the samples are homogeneous. The results showed silica source has a critical importance on the growth behavior of ZSM-5 zeolite, although the initial batch composition is very different.

3.3 N_2 adsorption

The N_2 adsorption-desorption isotherms (not shown) of the ZSM-5 nanocrystals exhibit a typical type I isotherm in accordance with IUPAC classification. Table 2 gives the details of the BET surface area and pore volume of the ZSM-5 nanocrystals with different silica source as obtained by the N_2 adsorption and desorption isotherms. Some trends were observed for the data in Table2. In the test range, the micropore surface area and micropore volume of the samples increased

depend on the type of silica source (Silicic Acid(SA) >Collidal Silica(CS) >Fumed Silica(FS) >Tetra Ethyle Ortho Silicate(TEOS)), which can be attributed to a highly polymeric silica and crystal growth rate compared to nucleation rate so that the resulting crystals have a larger size and a wider particle size distribution. However, use of silica source like TEOS that a low degree of polymerization favors' the formation of monodisperse ZSM-5. This result was effected in aluminum content depend so a higher Al-O bond length (0.175 nm) relative to the Si-O bond length (0.161 nm) (show table 1). An increase in the unit cell volume data, as observed by XRD, suggests that the pore dimensions increase after preparation by SA than TEOS related to greater amount of Al atoms. Therefore, the ZSM-5 nanocrystals with prepared by SA provided materials with the higher micropore volume. This result is in good agreement with the unit cell volume data obtained by XRD. The increased external surface area of the sample prepared by silicic acid as silica source can be attributed to the reduction of the individual crystal sizes of the ZSM-5 zeolites and the formation of more secondary mesopores.

In estimation of the pore size distribution of mesoporous materials by nitrogen adsorption measurements, the Dollimore–Heal method[36], which considers the thickness of mutilayer adsorption, provides a better estimation than the Barrett, Joyner & Halenda (BJH) method [36,37]. Pore size distribution curves of all samples were calculated by Dollimore–Heal method which was applied on desorption branch of each isotherm[37]. Results are shown in Fig. 3. It can be seen that the distributions of mesopores are quite narrow and similar for all samples. Increase polymeric silica and crystal growth rate in sample SA, the pore size distribution of ZSM-5 broadened and the average pore diameter decreased, giving evidence of the retention of the regularity of mesopores to some extent.

3.4. FT-IR spectra of various samples

The FT-IR spectra of ZSM-5 prepared by different silica sources CS, SA, FS and TEOS samples in the range 450-1400 cm^{-1} are shown in Fig. 4. The result shows bands at 1235, 1148, 800, 554 and 466 cm^{-1}, which are assigned to different vibrations of tetrahedral and framework atoms in ZSM-5[38]. The bands at about 1148 and 466 cm^{-1} are due to internal asymmetric stretching vibration of Si–O–T linkage, whereas the bands at about 1235, 800, and 554 cm^{-1} are due to symmetric stretching of the external linkage and hence sensitive to framework structure [38,39] .On the other hand the band at 466cm^{-1} related of T–O (where T= Si or Al) bending vibration of the $(Si,Al)O_4$ internal tetrahedral unites which designated as TO_4 in the framework of ZSM-5 [40]. However, the relative increased of the band at 554 in SA sample indicating the complete crystalline structure ZSM-5 crystalline structure.

The IR absorption band at 466cm^{-1} (I_{450}) can be taken as indicative of the vibration of TO_4 units, and that at 554 cm^{-1} (I_{550}) is attributable to the vibration of 10-membered oxygen rings [41-44]. The relative intensity ratio I_{550}/I_{450} expresses a quantitative index of crystallinity around the oxygen rings of ZSM-5. As can be seen in Table 1, the results show that the ratio and consequently relative crystallinity

increased in the following order: ((Silicic Acid(SA) >Collidal Silica(CS) >Fumed Silica(FS) >Tetra Ethyle Ortho Silicate(TEOS)), which is in close agreement with results obtained from the XRD data.

3.4.1. FT-IR spectra of pyridine adsorption

In order to evaluate the fate of acid sites in ZSM-5 samples, FT-IR spectra of pyridine adsorption were obtained (Fig. 5). The assignment of the bands has been given by Parry [45]. The bands at 1622, 1596, 1579 and 1444 cm^{-1} are ascribed to Lewis-coordinated pyridine (LPy), whereas the bands at 1651, 1632 and 1542 cm^{-1} are due to Brønsted-coordinated pyridine (BPy). The band at 1490 cm^{-1} is due to Lewis and Brønsted-coordinated pyridine (LPy + BPy).

A comparison between FT-IR spectra of pyridine adsorption on ZSM-5 samples at 150ºC shows increased in intensity in a band at 1444 cm^{-1} in samples FS and TEOS compared by CS and SA. This increased related to presence of strong Lewis acid sites, presumably formed by octahedrally coordinated aluminum species. This phenomenon appeared with presence band related to Brønsted acid sites in CS and SA at 1542 and 1651$cm^{-1}$with disappeared in FS and TEOS.

3.5. Adsorption of IC in aqueous solution by ZSM-5

3.5.1. Effect of contact time

Time taken to attain equilibrium is an important parameter to predict the efficiency and feasibility of an adsorbent when it is used for water pollution control. The adsorption of IC solution (100 ml), initial concentration 10ppm; pH = 4, onto ZSM-5 prepared by SA was studied as a function of contact time in order to determine the point of equilibrium as shown in Fig. 6. The adsorption capacity increased with increasing IC concentration in the medium. However, the adsorption procedure was almost completed during the first 90 min and the adsorption equilibrium was reached after 180 min. This result can be explained by the fact that the mode of adsorption of IC onto this sample is a typical physical adsorption. The rapid adsorption process is a most important feature in physical adsorption. According to this consequence, an optimum equilibrium at 90 min was selected for the adsorption isotherm experiments.

3.5.2. Effect of pH

Since the efficiency of sorption processes is strongly dependent on the pH, which affects the degree of ionization of dye as well as the surface properties of the sorbent, comparative experiments were performed at four pH values: 2, 4, 8, and 10. Fig. 7 show the effects of pH on the sorption process of IC dye on ZSM-5 prepared by SA. This figure clearly shows that the removal rate of IC was markedly enhanced at lower pH values, specifically at 4. It must be noted that the surface of the adsorbent changes its polarization according to the value of the pH of the solution and to the isoelectric point (IEP) of the solid [46,47]. Thus, the pH influences at the same time both the surface state of the adsorbent and the ionization state of ionizable organic molecules.

$$pH < IEP : Z\text{-}OH + H^+ \leftrightarrow Z\text{-}OH_2^+$$

$$pH > IEP : Z\text{-}OH + OH^- \leftrightarrow Z\text{-}O + H_2O$$

Since IC exposes negatively charged sulfonate SO_3^- groups, it is conceivable that at low pHs, its adsorption is favored. At pH < IEP, the surface is positively charged and many anions are competing.

3.5.3. Effect of ZSM-5 loading on decolorization efficiency of indigo carmine

Experiments were performed to study the variations in the rate of decolorization at different amount ZSM-5 prepared by SA as source of silica ranging from 0.5 to 2g/L as shown in Fig. 8. It was observed that the degree of decolorization efficiency of IC solution increases with increasing the amount ZSM-5, till 1g. The most effective decolorization of IC (80%) was observed with the ZSM-5 amount equal to 1g. after which (1.5 and 2g of ZSM-5) the decolorization efficiency decreases.

They concluded that the increase of ZSM-5 amounts promote the existence of the presence of parallel paths associated with catalyst degradation during the ZSM-5 cycle [e.g. dimerisation reaction] [49], and thus, increases as the concentration of the amount of a ZSM-5 increase. However, attaining complete decolorization of the dye at specific amount ZSM-5 (1g) nullifies the possibility of the presence of competing paths for the reaction and indeed suggests a facile pathway for decolorization of such a dye.

4. Conclusion

ZSM-5 adsorbent has been synthesized by using a hydrothermal method with different silica sources lead to changes in the properties of final product. ZSM-5 synthesized has been further examined for the adsorption behaviors of indigo carmine dyes. The physical and chemical properties of the resulting zeolite thus obtained in the study were characterized mainly based on the analyses of the nitrogen isotherms, scanning electron microscope (SEM) image, X-ray diffraction (XRD) pattern, FT-IR spectra and determination of acidity by pyridine adsorption. It was found that:

- The crystallinity % and Unit cell of ZSM-5 produced increased in the following order: Tetraethyleorthosilicate (TEOS) > Silicic Acid (SA) > Collidal Silica(CS) > Fumed Silica(FS).
- The micropore surface area and micropore volume of the samples increased depend on the type of silica source (SA > CS > FS > TEOS), which can be attributed to a highly polymeric silica and crystal growth rate compared to nucleation rate so that the resulting crystals have a larger size and a wider particle size distribution.
- SEM data show that single crystals obtained from SA are rounded-edged hexahedrons. When change of silica source from silicic acid to tetraethylorthosilicate leads to the formation of hexagonal twinned crystals with larger size and hemispherical raspberry when change silica by FS or CS.

- The adsorption of IC on ZSM-5prepared by SA was considerably higher than ZSM-5 prepared by TEOS or CS or FS and well regulated by pH. This was due to increasing high surface to volume ratio and the facile diffusion of IC onto the catalyst particle followed by its allocation into internal surfaces.

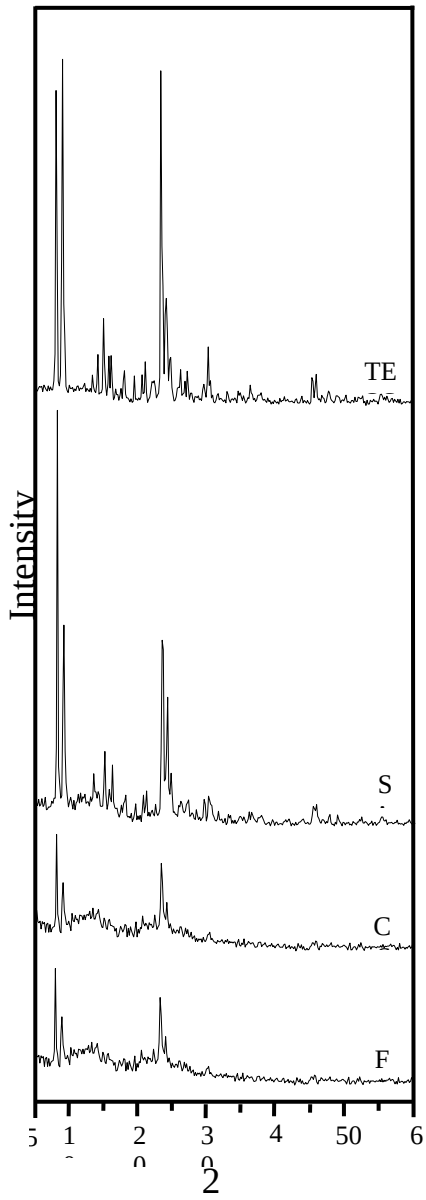

Fig. 1: X-ray diffractograms of ZSM-5 prepared by different silica sources.

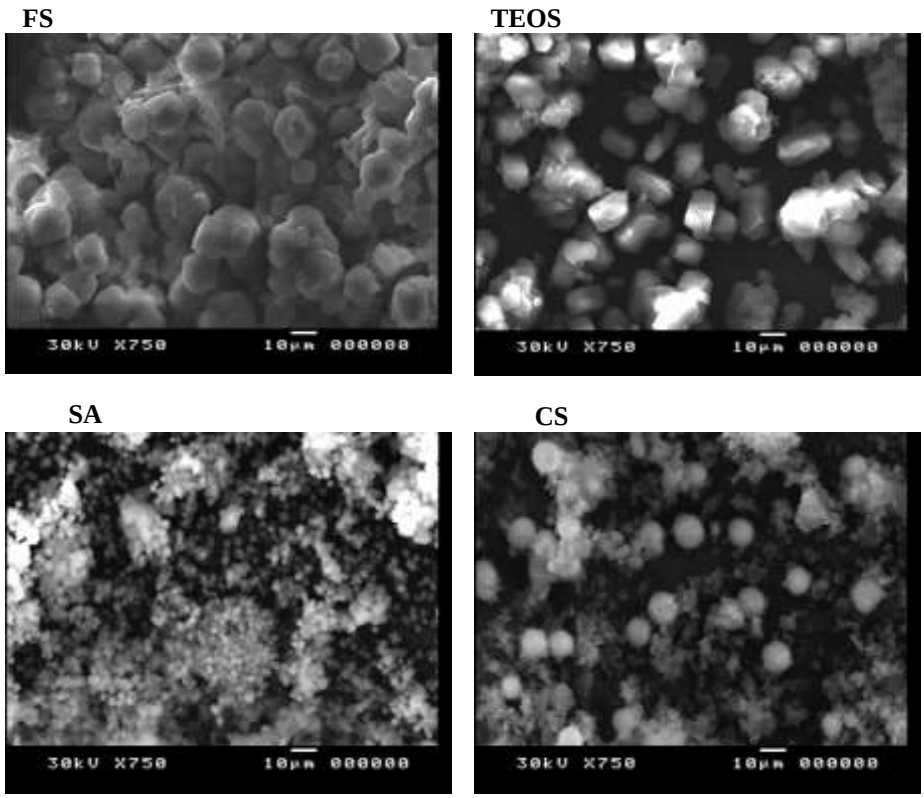

Fig. 2: The SEM micrographs depicting the topographical features of freshly activated ZSM-5 prepared by different silica.

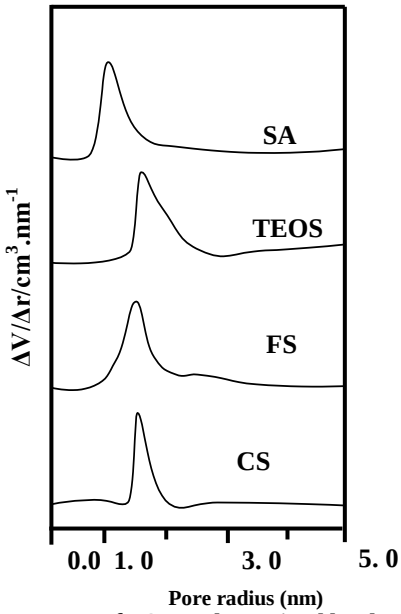

Fig. 3: Pore size distribution curves of ZSM-5 determined by the Dollimore–Heal method applied on the adsorption branch of the N_2 sorption isotherm.

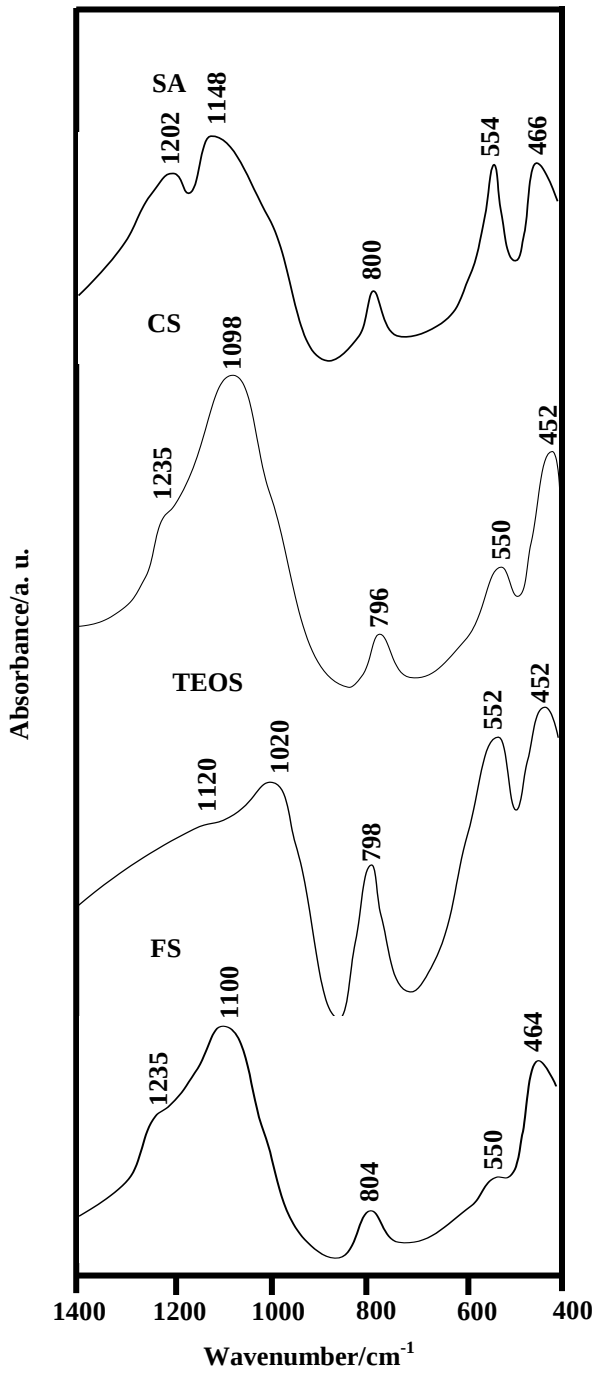

Fig.4: FTIR spectra of ZSM-5 prepared by different silica sources

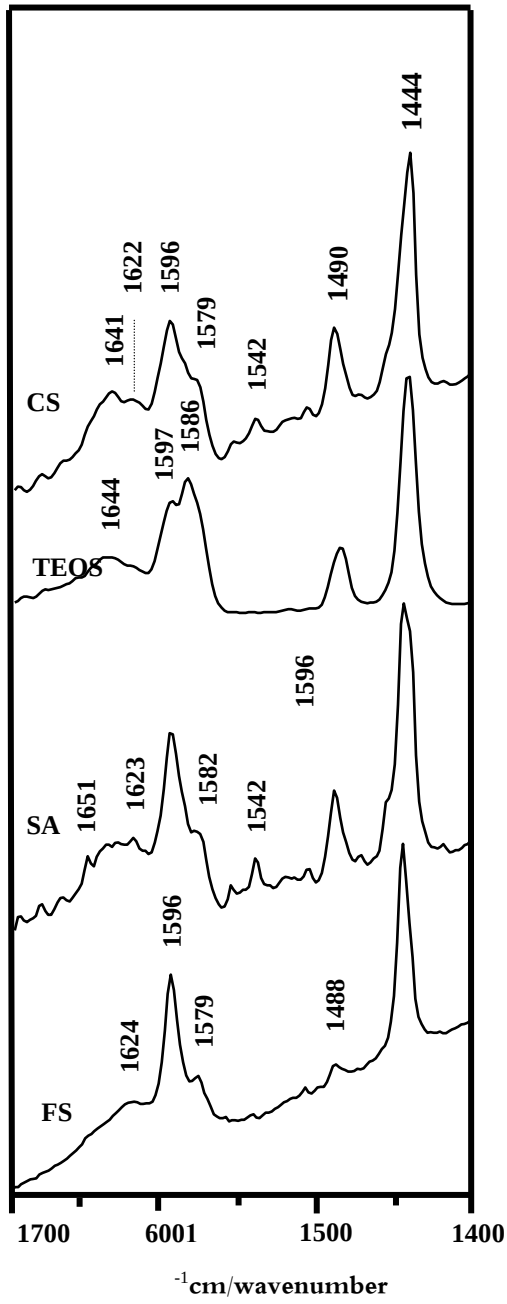

Fig.5: FT-IR spectra of pyridine adsorption on ZSM-5 prepared by different silica. Pyridine was introduced at room temperature and the spectra were recorded after evacuation at 100 ºC for 15 min.

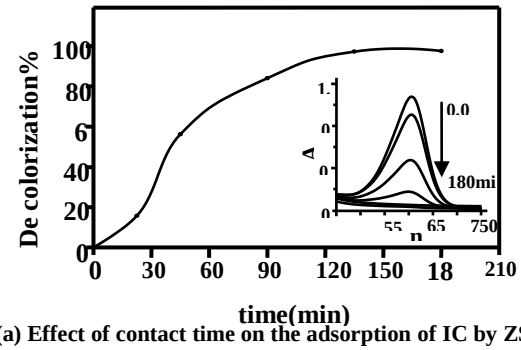

Fig.6: (a) Effect of contact time on the adsorption of IC by ZSM-5: initial IC concentration 10 ppm; pH 4; adsorbent dosage, 2 g/L.
(b) UV–Vis spectra of the effect of contact time on the adsorption of IC by ZSM-5

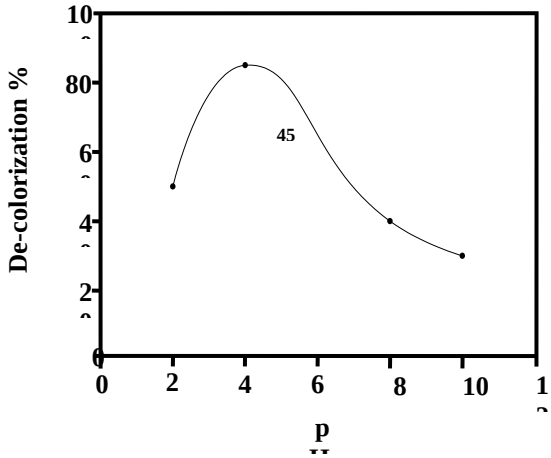

Fig.7: **Effect of pH on the adsorption of IC on ZSM-5**

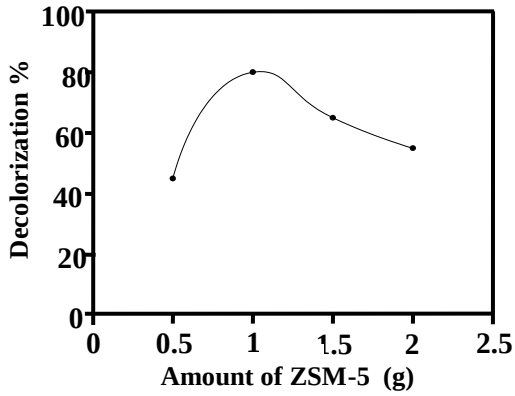

Fig. 8. Effect of ZSM-5 loading on the decolorization of IC.

Table1. Effect of silica sources on the crystallinity, particle size and unit cell parameters of ZSM-5 zeolite

Silica source	D (Å)	Unit cell parameters (Å)			V $(Å)^3$	XRD Crystallinity with respect to peak height/area	Crystal. by FT-IR %
		a	b	c			
CS	84.68	20.247	19.975	13.261	5363.20	40/28	53
FS	68.97	20.369	19.995	13.284	5410.28	15/19	25
TEOS	58.7	20.421	20.289	13.263	5495.15	100/100	100
SA	77.3	20.012	19.976	13.418	5363.98	62/58	71

Table 2: BET and pore volume of ZSM-5 nanocrystals with different silica source

Silica source	Surface area (m^2/g)			Pore volume (cm^3/g)		
	BET[a]	Micropore[b]	External[c]	total[a]	Micropore[b]	Mesopore
CS	798	664	134	0.78	0.617	0.163
FS	774	646	128	0.76	0.604	0.156
TEOS	698	575	123	0.71	0.543	0.167
SA	857	683	174	0.80	0.509	0.291

[a]BET method, [b]t-plot method, [c]Volume adsorbed at $p/p^0 = 0.95$

References

1. J. Grzechulska, A.W. Morawski, Appl. Catal. B 36 (2002) 45.
2. F.J. Green (Ed.), The Sigma Aldrich Handbook of Stains, Dyes and Indicators Aldrich Chemical, Milwaukee, WI, 1990, p. 403.
3. I. Arslan, I.A. Balcioglu, Dyes Pigments 43 (1999) 95.
4. P. Forlano, J.A. Olable, J.F. Magallans, M.A. Blesa, Can. J. Chem. 75 (1997) 9.
5. V.I. Parvulescu, D. Dumitru, G. Poncelet, J. Mol. Catal. A 140 (1999) 91.
6. O.P. Pestunova, G.L. Elizarova, V.N. Parmon, Russ. J. Appl. Chem. 72 (1999) 1209.
7. G. Centi, S. Perathoner, T. Torre, M.G. Verduna, Catal. Today 55 (2000) 61.
8. J.T. Spadaro, L. Isabelle, V. Renganathan, Environ. Sci. Technol. 28 (1994) 1389.
9. R.M. Barrer, Hydrothermal Chemistry of Zeolites, Academic Press, London, 1982.

10. D.W. Breck, Zeolite Molecular Sieves, Wiley, London, 1974.
11. M. Ryo, Y. Wada, T. Okubo, T. Nakazawa, Y. Hasegawa, S. Yanagida, J. Mater. Chem. 12 (2002) 1748.
12. C. Platas-Iglesias, L. Vander Elst, W.Z. Zhou, R.N. Muller, C. Geraldes, T. Maschmeyer, J.A. Peters, Chem. Eur. J. 8 (2002) 5121.
13. N.B. Castagnola, P.K. Dutta, J. Phys. Chem. B 102 (1998) 1696.
14. M. Lassinantti, J. Hedlund, J. Sterte, Micropor. Mesopor. Mater. 38 (2000) 25.
15. I. O. Ali, M. S. Thabet, K. S. El-Nasser, A. M. Hassan, T. M. Salama Micropor. Mesopor. Mater. 160 (2012) 97 -105.
16. I. O. Ali A. M. Hassan, S. M. Shaaban, K. S. Soliman, Sep.Purif. Techn. 83 (2011) 38
17. S. Mintova, S.Y. Mo, T. Bein, Chem. Mater. 13 (2001) 901.
18. L. Tosheva, V. Valtchev, Chem. Mater. 17 (2005) 2494.
19. A.E. Persson, B.J. Schoeman, J. Sterte, J.-E. Otterstedt, Zeolites 14 (1994) 557.
20. C.E.A. Kirschhock, R. Ravishankar, L. van Looveren, P.A. Jacobs, J.A. Martens, J. Phys. Chem. B 103 (1999) 4972.
21. O. Regev, Y. Cohen, E. Kehat, Y. Talmon, Zeolites 14 (1994) 314.
22. B.J. Schoeman, Micropor. Mesopor. Mater. 22 (1998) 9.
23. S.L. Burkett, M.E. Davis, Chem. Mater. 7 (1995) 920.
24. P.-P.E.A. de Moor, T.P.M. Beelen, R.A. van Santen, J. Phys. Chem. B 103 (1999) 1639.
25. Q. Li, D. Creaser, J. Sterte, Micropor. Mesopor. Mater. 31 (1999) 141.
26. W.H. Dokter, H.F. Garderen, T.P.M. Beelen, R.A. Santen, W. Bras, Angew. Chem. Int. Ed. Engl. 34 (1995) 73.
27. M. Tsapatsis, M. Lovallo, M.E. Davis, Micropor. Mater. 5 (1996) 381.
28. B.J. Schoeman, E. Babouchkina, S. Mintova, V. Valtchev, J. Sterte, J. Porous Mater. 8 (2001) 13.
29. S. Mintova, N.H. Olson, T. Bein, Angew. Chem. Int. Ed. 38 (1999) 3201.
30. S. Mintova, N. Olson, V. Valtchev, T. Bein, Science 283 (1999) 958.
31. Q. Li, B. Mihailova, D. Creaser, J. Sterte, Micropor. Mesopor. Mater. 43 (2001) 51.
32. P. Scherrer, Goettingen Nachr 98 (1918) 2.
33. J.H. de Boer, B.G. Linsen, T.J. Osinga, J. Catal. 4 (1964) 643.
34. COEI-3-REASOL, International Oenological Codex, Reagents and titrated solutions (2003)15
35. I.O. Ali, A.M. Hassan, S. M. Shaaban, K.S. Soliman Sep. Purif. Technol. 83 (2011) 38-44.
36. D. Dollimore, G.R.Heal, *J. Applied Chem*., **1964**, 14, 109-114.
37. D. Dollimore, G.R.Heal, *J. Colloid Interface Sci.*, **1970,** 33(4), 508-519.
38. V. Sundraramurthy, N. Lingappan, J. Mol. Catal. A 160 (2000) 367.
39. M.M. Mohamed, I. Othman, N.A. Eissa, Micropore Mesopore Mater. 87 (2005), 93.
40. M. Flanigen, Adv. Chem. Ser. 119 (1973) 121
41. K.F.M.G.J. Scholle, W.S. Veeman, P. Frenken, G.P.M. van der Velden, Appl. Catal. 17 (1985) 233.
42. J.C. Jansen, F.J. van der Gaag, H. van Bekkum, Zeolites (1984) 369.
43. O.G. Somani, A.L. Choudhari, B.S. Rao, S.P. Mirajkar, Mater. Chem. Phys. 82 (2003) 538.
44. I.O. Ali, Mater. Sci. Eng., A 459 (2007) 294–302.
45. E.P. Parry, J. Catal. 2 (1964) 371.
46. G. Poncelet, P.A. Jacobs, P. Grange (Eds.), Preparation of Catalysts V,Elsevier, Amsterdam, 1991.
47. M. M. Mohamed, J. Coll. Inter. Sci. 272 (2004) 28–34
L. Canali, D. C. Sherrington, Chem. Soc. Rev. 28 (1999) 85.